ACS APPLIED MATERIALS & INTERFACES

Research Article

www.acsami.org

Graphene Oxide as a High-Performance Fluid-Loss-Control Additive in Water-Based Drilling Fluids

Dmitry V. Kosynkin,[†,‡] Gabriel Ceriotti,[†,‡] Kurt C. Wilson,[†,‡] Jay R. Lomeda,[†,‡] Jason T. Scorsone,[∥] Arvind D. Patel,[∥] James E. Friedheim,[∥] and James M. Tour*[,†,‡,§]

[†]Department of Chemistry, [‡]Richard E. Smalley Institute for Nanoscale Science and Technology, [§]Department of Mechanical Engineering and Materials Science, Rice University, 6100 Main Street, Houston, Texas 77005, United States

[∥]M-I SWACO, LLC, 5950 North Course Drive, Houston, Texas 77272, United States

Supporting Information

ABSTRACT: Graphene oxide (GO) performs well as a filtration additive in water-based drilling fluids at concentrations as low as 0.2 % (w/w) by carbon content. Standard American Petroleum Institute (API) filtration tests were conducted on pH-adjusted, aqueous dispersions of GO and xanthan gum. It was found that a combination of large-flake GO and powdered GO in a 3:1 ratio performed best in the API tests, allowing an average fluid loss of 6.1 mL over 30 min and leaving a filter cake ~20 μm thick. In comparison, a standard suspension (~12 g/L) of clays and polymers used in the oil industry gave an average fluid loss of 7.2 mL and a filter cake ~280 μm thick. Scanning electron microscopy imaging revealed the extreme pliability of well-exfoliated GO, as the pressure due to filtration crumpled single GO sheets, forcing them to slide through pores with diameters much smaller than the flake's flattened size. GO solutions also exhibited greater shear thinning and higher temperature stability compared to clay-based fluid-loss additives, demonstrating potential for high-temperature well applications.

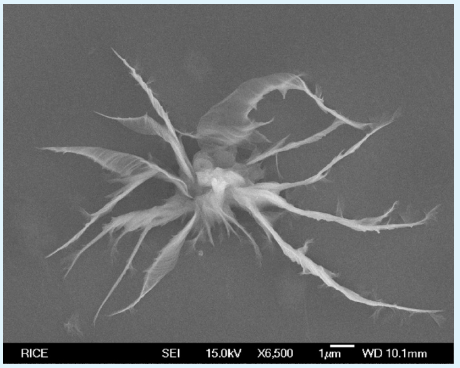

KEYWORDS: *graphene oxide, drilling fluid, shear thinning, oil well*

INTRODUCTION

Oil-drilling fluids, more commonly known as drilling muds, are complex chemical systems that are essential for oil-drilling excavation. Among other functions, an oil-drilling fluid needs to carry drill cuttings to the surface of the well, support the walls of the well bore, protect the producing formation from damage, cool and lubricate the drill bit, prevent drill-pipe corrosion, facilitate the acquisition of information about the formation being drilled, and create a thin low-permeability cake that protects permeable production formations. Fluid invasion into porous formations can damage reservoirs and reduce productivity by blocking hydrocarbon exit flow paths or causing formation collapse. Fluid-loss-control additives form filter cakes surrounding the wellbore to retard the loss of drilling fluid into permeable formations. Ideal additives form a stable dispersion in brine solutions and are effective at low concentrations. Currently, most filtration-loss-prevention additives in water-based muds (WBMs) have formulations based on clay, lignite, asphaltite, or organic polymers, with bentonite clays being very common.[1−4]

Graphene, as a single layer of graphite, has become the subject of much research interest for its unique materials properties.[5,6] Among other interesting features, a pristine graphene monolayer has a theoretical Connolly surface area of 2965 m^2/g and has been shown to form a membrane impermeable even to helium gas.[7,8] Graphene might make a good candidate as a pore-plugging filter in oil-drilling fluids. However, the difficulty of dispersing large graphene flakes in aqueous media[9] creates problems in WBMs. Instead, oxidized graphene provides a more stable material for aqueous dispersions and it maintains the sheet-like morphology that would allow the desired pore-plugging through filtercake formation (Figure 1).[10]

Graphene oxide (GO) is commonly obtained from an aqueous dispersion of graphite oxide. Graphite oxide was first synthesized by Brody in the 19th century by carefully reacting natural graphite with oxidizing agents in a solution of oxidizing acids.[11] In solution, graphite oxide exfoliates into oxidized carbon monolayers that are considerably more soluble in water than is pristine graphene. Much of the research currently done with GO involves deliniation of methods for its reduction to graphene,[2] with additional work studying applications for GO itself.[12] For example, dispersed GO flakes can be sifted out of solution and pressed in order to make a strong paper-like material, which results from a robust tile-like interlocking of the flakes.[13,14] This could be beneficial for making a thin

Received: September 19, 2011
Accepted: December 2, 2011
Published: December 2, 2011

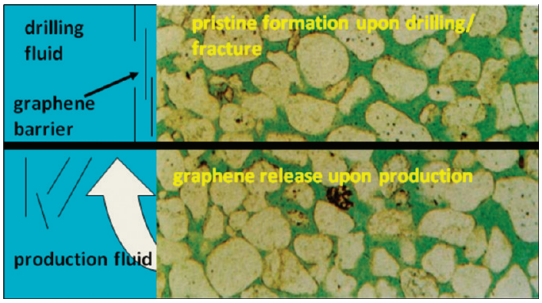

Figure 1. While drilling, as the pressure is high (upper figure), the graphene sheets form a film to prevent the infiltration of the drilling fluids into the pristine formation. Upon lowering the pressure in the wellbore during recovery (lower figure), the oil and gases in the formation push the graphene sheets off the bore wall.

impermeable film to prevent fluid loss in the wellbore. Since GO sheets are well-exfoliated, they could be used at substantially lower concentrations than clay-based additives to obtain the desired performance. More importantly, the nanometer thickness of the GO flakes could also result in much thinner filter cakes than those obtained using clay-based materials. The thickness of a wellbore's filter cake is directly and strongly correlated to the differential torque needed to rotate the pipe during drilling, to the drilling time, and to drilling costs.[15] GO is further appealing in that it offers the prospect of an environmentally friendly[16] and inexpensive[17] technology.

Natural and synthetic graphite are inexpensive feedstocks for GO production, with the potential for industrial-scale synthesis through procedures developed by Brodie,[11] Staudenmaier,[18] Hummers,[19] and others.[20,21] In addition, a growing body of knowledge related to the chemical modification of GO offers means for tuning its materials properties to achieve better performance in drilling fluids.[22−26] For example, esterification of GO can make it more stable in saline solutions. Although GO precipitates in highly saline solutions, methylated GO (MeGO) has been used in high salinity waterflooding media (used to wash stranded hydrocarbon deposits from reservoirs).[27]

In the present study we investigate the suitability and potential performance of GO and its derivatives as compared with commonly used fluid-loss-control agents in fresh water muds (FWMs). Additionally, the performance of MeGO in saltwater muds (SWMs) is explored.

EXPERIMENTAL SECTION

Preparation of Powder and Large-Flake GO. Powder GO (PGO) and large-flake GO (LFGO) were synthesized using the same procedure, with the only difference being the starting carbonaceous material. PGO was derived from microcrystalline synthetic graphite (< 20 μm sheets) and LFGO from graphite flakes (+100 mesh), both from Sigma-Aldrich. In a typical synthesis, the carbon precursor (30 g) was added to a 1 L Erlenmeyer flask. H_2SO_4 (540 mL, 96.6 % w/w, Fischer Scientific) and H_3PO_4 (60 mL, ≥ 85%, Sigma-Aldrich) (i.e., 600 mL of 9:1 H_2SO_4/H_3PO_4) and the first of five portions of $KMnO_4$ (30 g each, 99%, J.T. Baker) were added to the flask, and the mixture was stirred with a glass rod for 5 min. The remaining $KMnO_4$ portions were added approximately every 12 h until all of the $KMnO_4$ was added; each addition was accompanied by 5 min of stirring with a glass rod. As more $KMnO_4$ was added and the graphite was exfoliated, the mixture thickened. The vessel was covered with a piece of aluminum foil in between additions and stirrings. 12 h after adding the last portion of $KMnO_4$, the reaction was quenched by pouring the mixture into a 2 L beaker filled with ice (500 g). H_2O_2 (30% w/w Fischer Scientific) was added, 1 mL at a time, with stirring in between additions, onto the quenched mixture until it was a constant golden-yellow color and gas evolution ceased. The total H_2O_2 addition was ~15 mL. The process described is similar to our previously published procedure for synthesis of GO.[20] The concentration of $KMnO_4$ added at any time to the H_2SO_4 solution was 5% wt/vol. A new portion of $KMnO_4$ was not added until the green Mn_2O_7 species was observed to have disappeared. **Caution: Do not exceed ~5% wt/vol, and do not apply heat; it is reported that, at concentrations of 7% wt/vol $KMnO_4$ in H_2SO_4, the mixture can explode upon heating.**[28] To purify the product, the solution was repeatedly centrifuge-washed before filtering. The quenched solution was evenly distributed among four 250 mL polypropylene centrifuge bottles (Nalgene, NY, U.S.A.) and centrifuged (Sorvall T1, Thermo Scientific) at 4000 rpm for 90 min. The supernatant was discarded, and the precipitate re-suspended by shaking with DI H_2O (200 mL) in each bottle. This process of precipitation and re-suspension was repeated again with DI H_2O, 10% HCl (Sigma-Aldrich), and twice with anhydrous ethanol (200 proof, Decon Labs Inc.). Finally, the precipitate was resuspended in anhydrous ethyl ether (200 mL, 99.9%, Fischer Scientific) and filtered over a 0.45 μm pore size PTFE membrane to obtain clean GO. The filter cake was ground into a fine powder with a mortar and pestle, and the ether was allowed to evaporate at room temperature in a fume hood overnight.

Preparation of Methylated LFGO and PGOs. To esterify acidic functional groups and improve stability in saline solutions in accordance to published procedures,[14] methylated LFGO (MeLFGO) and methylated PGO (MePGO) were synthesized. Both materials were synthesized using the same method with only the GO precursor being different in each reaction. In a standard run, the selected GO (30 g) was heated at reflux (65 °C) with stirring in methanol (200 mL, ≥99.8% from Sigma Aldrich) with conc. H_2SO_4 (4 drops) for 4 d. After cooling to room temperature, the suspension was centrifuged (4000 rpm for 45 min), the supernatant discarded, and the precipitate re-suspended in fresh methanol (200 mL). This suspension was centrifuged, and the supernatant discarded. The precipitate was re-suspended in anhydrous ethyl ether (200 mL) and filtered over a 0.45 μm pore size PTFE membrane. The resulting cake was ground into a fine powder with a mortar and pestle, and the ethyl ether was allowed to evaporate at room temperature in a fume hood overnight.

Determination of %C Content by Chemical Reduction. To determine the %C content of a sample, the GO (1 g) was dispersed in deionized water (100 mL) while stirring in a 100 mL round bottom flask using a PTFE-coated stir bar. Once the GO was dispersed, hydrazine hydrate (0.2 mL) was added to the mixture. The mixture was then heated with stirring to 95 °C for 1 h in a flask equipped with a reflux condenser. Conc. HCl (0.2 mL) was added to the solution in order to precipitate the reduced carbon (pH 2). Finally, the precipitate was filtered, and the filter cake was subsequently washed with methanol and ether. The filtered sample was dried under vacuum (3−4 Torr) at 95−100 °C and weighed. Carbon content was calculated as the ratio of the starting weight to the weight of dried precipitate. The percentage carbon content (%C) of the materials used was as follows: PGO, 30.0%; LFGO, 5.2%; MePGO, 16.0%; MeLFGO, 19.0%.

Sample Preparation for API Fluid-Loss Test. Xanthan gum is a common rheological modifier that can be used in both FWMs and SWMs for increased viscosity and better dispersion stability. As such, tap water viscosified with xanthan gum was selected as the base for the GO suspensions investigated in this study. Solutions of 0.75 lb per barrel (lb/bbl, ~2.89 g/L) xanthan gum (provided by MI SWACO under the trade name DUOVIS) were made by mixing the material with tap water while heating to 95 °C and stirring for 1 h. When saline solutions were needed, they were made by adding NaCl (120 g/L, 99%, Fischer Scientific) to the DUOVIS suspension before adding the GO. To standardize results between different GO samples, GO was added to 100 mL samples of the xanthan gum solution on the basis of carbon content (e.g., if LFGO has a %C content of 5.2%, a LFGO solution of 2 g/L carbon-content would have a total of 38.5 g/L of LFGO). The GO mixture was dispersed with a mechanical homogenizer (Ultra-Turrax T25 from IKA) for 15 min at 10 000

dx.doi.org/10.1021/am2012799 | ACS Appl. Mater. Interfaces 2012, 4, 222−227

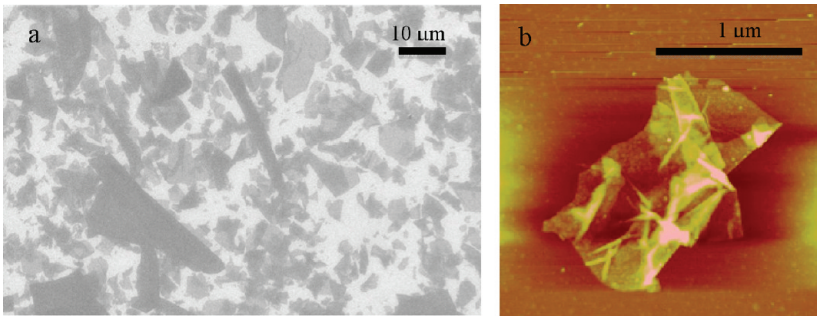

Figure 2. (a) SEM of LFGO flakes and (b) AFM micrograph of a PGO flake.

rpm. The dispersion was then adjusted to pH 9−10 by dropwise addition of 50% w/w NaOH solution while monitoring the pH with a digital pH meter. All GO suspensions mentioned henceforth are additions of GO on the basis of %C to viscosified tap water.

API Fluid-Loss Test Conditions. Fluid-loss tests followed API guidelines for water-based fluids.[29] Tests were conducted in a standard API apparatus using Whatman quantitative filter paper, hardened low-ash Grade 50 (estimated pore size 2.7 μm). All filtration loss tests were conducted at 20 °C. In a standard run, 100 mL of 2 g/L GO solution were placed in the apparatus with 100 psi differential pressure supplied by argon gas across a filter paper. Filtrate volumes were then measured at 1.0, 7.5, 15.0, 20.0, and 30.0 min after starting the test. The filter paper was then removed, lightly washed, and set out at room temperature for 12−24 h to allow for the water to evaporate from the filter cake. Weight was applied on the edges of the filter paper to prevent it from curling upon drying. After the filter cake was stiff enough to permit measurement, its thickness was determined using a micrometer accurate to ±1 μm.

Instrumental Analyses. X-ray photoelectron spectroscopy (XPS) was performed on a PHI Quantera SXM scanning X-ray microprobe with a 26.00 eV pass energy, 45 °C take-off angle, and 100 μm beam size. Samples were prepared by pressing dry GO powder on an In film. Thermogravimetric analyses (TGA) were performed on a Q50 TA Instrument analyzer under 98% purity argon gas and temperatures ramping from 30 to 950 °C at a rate of 5 °C/min except at 1 °C/min between 120 and 400 °C. Scanning electron microscopy (SEM) was performed using an FEI Quanta 400 high-resolution field emission scanning electron microscope in high vacuum mode. Samples were prepared by suspending the dry GO in water and spin-coating it on a SiO_2 substrate at 3000 rpm. Atomic force microscopy (AFM) was used to obtain topographic images of GO. A Nanoscope Illa (Digital Instrument/Veeco Metrology) under tapping mode, with a scan rate of 1 Hz and Si tips n-doped with 1-10 Ω•cm phosphorous (Veeco MPP-11100-140), was used. Samples were prepared by spin coating aqueous solutions of GO materials at 3000 rpm for 10 min on top of mica surfaces (Ted Pella). Rheometry was performed using a Fann Viscometer model 35A. Solutions were kept at 120 °F (~50 °C), and API guidelines for field-testing of drilling fluids were followed at all times.[29]

RESULTS AND DISCUSSION

Sample Characterization. Electron micrographs of GO flakes were obtained by transferring samples onto silicon dioxide coated highly doped silicon substrates. The scanning electron microscope (SEM) micrographs in Figure 2 show a large variance in particle diameter. AFM images reveal sheet-like surface morphologies with most flakes folded in multiple locations. When dispersed in aqueous solutions, GO forms nematic (discotic) liquid crystals (Figure S1 in the Supporting Information). GO particles can be seen aggregating into clumps of aligned sheets like stacks of paper. This self-aligning property should assist the filtration characteristics of GO dispersions.

It is important to have additives for WBMs that are stable in saline environments, as many mud formulations (such as SWMs) lower the osmotic pressure gradient across the bore-wall membrane by increasing the salinity of the drilling fluid. Unmodified GO was found to aggregate and precipitate from electrolyte solutions with divalent cation (Ca^{2+} and Mg^{2+}) concentrations as low as 0.001 M. This is thought to be due to the anionic carboxyl groups on the edges and the acidic hydroxyl groups on the planes of the GO sheets bonding with the cations to form large aggregates that separate from solution.[30] As a result, in order to prevent their coagulation, PGO and LFGO were heated with methanol in the presence of H_2SO_4 to esterify the carboxylic acid groups and form methyl ethers from the hydroxyl groups, producing methylated PGO (MePGO) and MeLFGO. To determine the extent of methylation that resulted from the procedure employed, MeLFGO (1 g) was treated with a large excess (> 200 mL) of 2-chloroethanol under the same esterification conditions as those used for the methylation to replace the methoxy groups with 2-chloroethoxy substituents that are detectable by XPS. The chlorinated sample was then analyzed by XPS, revealing 1.5% chlorine content (Figure S2). The degree of chlorination was considered to be equal to the amount of methylation in the MeLFGO sample. The resulting MeLFGO and MePGO exhibited greater saline stability in 1.0 M $CaCl_2$ solution than the original LFGO (Figure 3) and PGO, proving that a small change in surface chemistry can vastly improve GO's stability in saline solution.

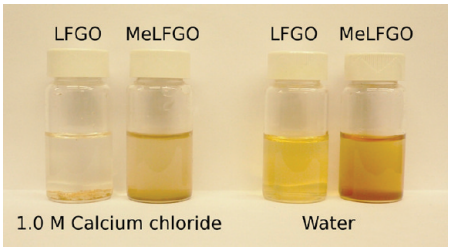

Figure 3. 10 mg suspensions of LFGO and MeLFGO in 15 mL of 1.0 M $CaCl_2$ solution and in tap water. When dispersed in $CaCl_2$ solution, the LFGO particles immediately flocculated and precipitated from solution, resulting in lower opacity, while the majority of the MeLFGO stayed in suspension.

GO solutions underwent rheological testing to determine viscosity and shear thinning properties. An aqueous suspension of LFGO at a concentration of 2.7 mg/mL demonstrated shear thinning properties (Figure S3). This solution exhibited a dynamic viscosity of ~3500 cP at rest, but shear thinning resulted in a viscosity <5 cP at 6000 rpm. Shear thinning fluids

are more easily pumped downhole and are highly desirable in the field.

TGA was performed on samples of LFGO and MeLFGO prepared from flake graphite. After a 30 min isotherm at 120 °C to fully dehydrate the sample, the temperature was increased by 1 °C/min to 400 °C, and then by 5 °C/min to 950 °C in an argon/nitrogen atmosphere. At faster rates of heating, the samples frequently rapidly expanded out of the TGA pan due to rapid deoxygenation.[31] Methylation appears to raise the threshold for initial thermal decomposition by 10−20 °C compared to PGO and LFGO. Figure 4 shows how MeLFGO

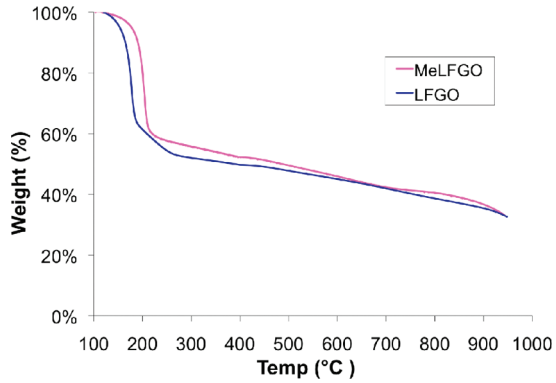

Figure 4. TGA of LFGO and MeLFGO sample. MeLFGO appears to have a higher threshold for initial thermal decomposition.

drops from 98% of original sample weight to 60% over the temperature range of 155 to 220 °C, while LFGO falls from the same weight % values in the temperature range of 140 to 210 °C. High temperature stability is an important feature for fluid-loss-control additives because many of the organic polymers commonly used thermally decompose above 120 °C, while clays undergo hydrolysis, resulting in destruction of silica sheets and loss of barrier forming properties.[4]

Filtration Properties. Suspensions of GOs in viscosified water were evaluated by API fluid-loss tests. It was found that the first 5 mL of fluid-loss filtrate from LFGO solutions was a dark viscous liquid. The remaining filtrate was colorless. SEM imaging of the dark filtrate revealed that individual sheets of LFGO passed through pores much smaller than the diameter of the flattened LFGO by crumpling and folding into starfish shapes (Figure 5). Molecular modeling confirms and explains the extreme pliability of GO.[32]

Solutions composed of LFGO exhibited good filtration properties after quickly passing an initial volume of filtrate. At 2 g/L of LFGO with xanthan gum (2.9 g/L), LFGO exhibited a filtration rate of less than 0.1 mL/min after 15 min (Figure 6).

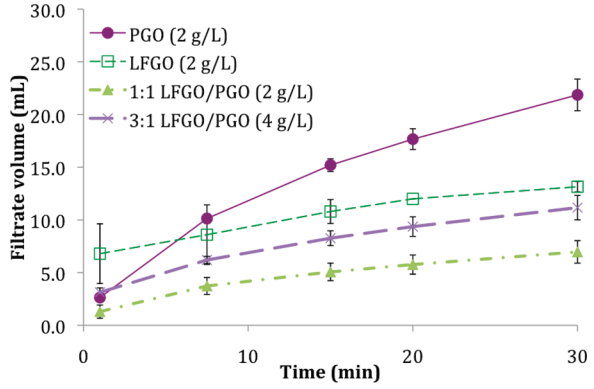

Figure 6. API filtration loss results for LFGO, PGO, a 1:1 mix and a 3:1 mix of LFGO and PGO suspensions at 2 g/L carbon-content concentrations in 2.9 g/L (0.75 lbm/bbl) xanthan gum solution.

In contrast, PGO derived from synthetic graphite powder (<20 μm) displayed less initial filtration loss, but overall worse performance. This difference is thought to be a result of the surface morphologies of the two graphite sources, with internal cross-linking between layers in the synthetic graphite powder preventing full exfoliation of the GO particles from which it is derived.

We hypothesized that prevention of the LFGO from folding by the addition of less pliable particles that showed good adhesion to GO would reduce the amount of the initial fluid loss. A recent molecular dynamics study showed the high affinity of GO to itself and to other particles due to interparticle hydrogen bonding.[33] A smaller, more rigid particle (such as smaller flake GO) mixed with LFGO might act as a reinforcer of the cake-coating porous formation. Indeed, PGO mixed with LFGO (1:1 wt and 3:1 wt ratios) gave noticeably better filtration properties, (Figure 6). The hydrogen bonding between the oxygen-containing functional groups on the surfaces of the two types of GO are likely responsible for the superior filtration characteristics. After investigating combinations of 1:3, 1:1, 3:1, 1:7, and 3:5 w/w LFGO/PGO at 4 g/L loads, a 3:1 w/w LFGO/PGO mixture as weighted by carbon content was found to give the optimal ratio for filtration-loss-control properties. Synthetic graphite powder was investigated as a reinforcing agent in place of PGO, but it did not perform as well as PGO when mixed in LFGO formulations (Figure S4).

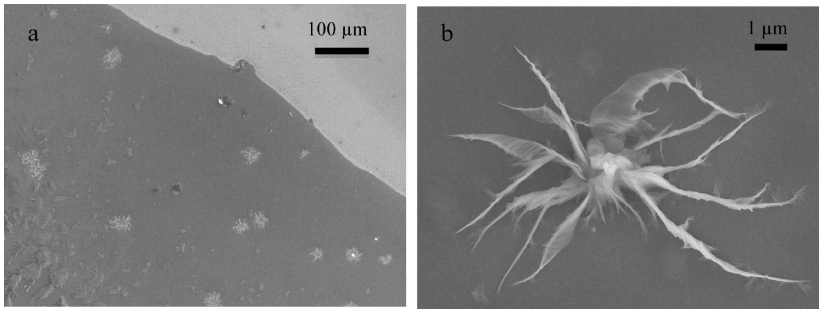

Figure 5. SEM images of (a) multiple LFGO flakes folded into starfish shapes and (b) a single such particle that entered into a 2.7 μm diameter pore with 100 psi of applied pressure.

dx.doi.org/10.1021/am2012799 | ACS Appl. Mater. Interfaces 2012, 4, 222−227

To compare the filtration properties of GO to currently available mud formulations, a representative typical mud formula, without drill cuttings, was obtained from M-I SWACO. This proprietary formula contained many dissolved solids in the form of bentonite and attapulgite clays along with ultralow viscosity polyanionic cellulose (PolyPAC UL) organic polymers as fluid-loss-control additives. The resulting M-I SWACO fluid is denser than the GO based fluid, 1.06 g/mL compared to 1.00 g/mL, respectively. A large amount of dissolved solids was not deemed necessary in the GO-based fluids because GO is a strong viscosifier at low concentrations, and there would be deleterious interactions between the GO and the dispersed clay. Solutions of GO at concentrations above 4 g/L became too thick to ensure proper dispersion.

The 4 g/L GO solution produced less filtrate volume and a slower final rate of filtration than the M-I SWACO bentonite + PolyPAC UL formulation (Table 1). Also, the filter cake from the GO solutions measured an order of magnitude thinner, at an average thickness of 22 μm, compared to 278 μm for the M-I SWACO fluid. A thin filter cake reduces friction in the well bore, which can be important to avoid pipe sticking and subsequent downtime while drilling. Additionally, the GO formulation contains less than half as many suspended solids by mass. Decreasing the concentration of suspended solids has been shown to increase the rate of penetration when drilling,[34] and there is furthermore less environmental impact.

Table 1. API Test Results of GO Solutions

Solution	Filtrate Volume (mL) (95% confidence)	Final Filtration Rate (mL/min)	Cake Thickness (μm) (95% confidence)
3:1 LFGO/PGO (2 g/L)	10.8 ± 0.7	0.18	19 ± 4
3:1 LFGO/PGO (4 g/L)	6.1 ± 0.5	0.11	21.6 ± 0.2
Bentonite + PolyPAC UL	7.2 ± 0.4	0.14	278 ± 65

To show the suitability of MeLFGO and MePGO as fluid-loss additives in saline solutions, filtration loss tests of 2 g/L by carbon content in 2.9 g/L xanthan gum solutions with 120 g/L NaCl were performed. From the experiment shown in Figure 3, it was expected that MeLFGO and MePGO would produce more stable suspensions than LFGO and PGO, thus leading to lower filtrate loss than LFGO and PGO. Indeed, the fluid-loss volumes of the MeLFGO and MePGO solutions were substantially less, as can be seen in Figures 7 and 8, respectively,

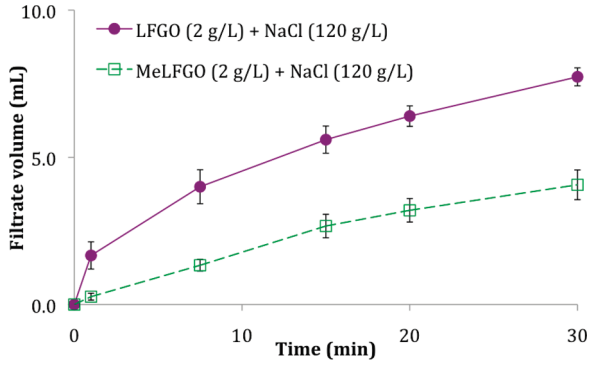

Figure 7. API filtration loss of LFGO and MeLFGO suspensions in 2.9 g/L (0.75 lbm/bbl) xanthan gum and NaCl (120 g/L) solutions.

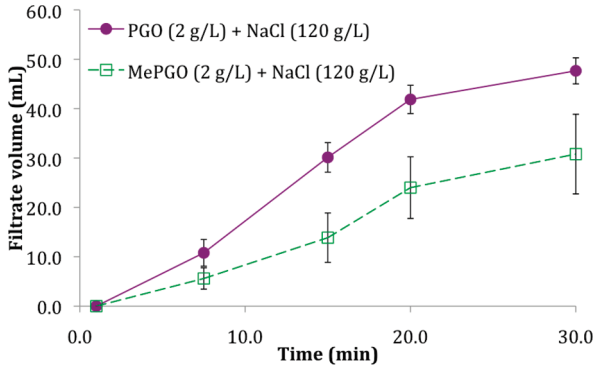

Figure 8. API filtration loss of PGO and MePGO suspensions in 2.9 g/L (0.75 lbm/bbl) xanthan gum and NaCl (120 g/L) solutions.

suggesting MeGO is a suitable alternative for GO in saline conditions.

CONCLUSION

We have shown that GO is an effective fluid-loss-control additive in WBMs. By methylating the GO through an esterification reaction, the stability of GO in saline environments is increased, leading to potential application in both FWMs and SWMs. GO prepared from natural graphite flakes passed through pores many times smaller than the particle's original diameter by folding into starfish shapes. By combining LFGO with PGO as a reinforcing agent, enhanced filtration properties were observed. At a concentration of 4 g/L by carbon content, the LFGO/PGO mixture had superior filtration properties when compared to a standard bentonite + PolyPAC UL formulation, yielding less filtration loss, a lower final filtration rate, and a substantially thinner filter cake. GO has the potential for industrial scalability through production from abundant graphite sources and common reagents. GO's unique properties make it an ideal candidate for the next generation of fluid-loss-control additives.

ASSOCIATED CONTENT

Supporting Information

Polarized light micrograph (Figure S1), XPS spectra (Figure S2), viscosity plot (Figure S3), fluid-loss plots of graphite reinforced suspensions of LFGO I xanthan gum solution (Figure S4), relative solution stability of PGO and MePGO in the presence of calcium chloride (Figure S5), and TGA analyses of PGO and MePGO. This material is available free of charge via the Internet at http://pubs.acs.org.

AUTHOR INFORMATION

Corresponding Author

*E-mail: tour@rice.edu.

ACKNOWLEDGMENTS

We thank A. Sinitskii for acquiring the SEM images that show the GO starfish. This work was funded by M-I SWACO, a Schlumberger Company.

REFERENCES

(1) Moore, P. L. *Drilling Practices Manual*; The Petroleum Publishing Co.: Tulsa, OK, 1974.

(2) *Standard Handbook of Petroleum & Natural Gas Engineering*; Lyons, W. C., Ed.; Gulf Publishing Co.: Houston, TX, 1996; p 1.

(3) Patel, A. D.; Stamatkis, E.; Davids, E. U.S. Patent 6,247,543, 2001.

(4) McDermott, J. *Drilling Mud and Fluid Additives*: Noyes Data Corp.: London, 1973.
(5) Geim, A. K. *Science* **2009**, *324*, 1530−1534.
(6) Allen, M. J.; Tung, V. C.; Kaner, R. B. *Chem. Rev.* **2010**, *110*, 132−145.
(7) Chae, H. K.; Siberio-Perez, D. Y.; Kim, J.; Go, Y.; Eddaoudi, M.; Matzger, A. J.; O'Keeffe, M.; Yaghi, O. M. *Nature* **2004**, *427*, 523−527.
(8) Bunch, J. S.; Verbridge, S. S.; Alden, J. S.; van der Zande, A. M.; Parpia, J. M.; Craighead, H. G.; McEuen, P. L. *Nano Lett.* **2008**, *8*, 2458−2462.
(9) Luo, J.; Conte, L. J.; Tung, V. C.; Tan, A. T. L.; Goins, P. E.; Wu, J.; Huang, J. *J. Am. Chem. Soc.* **2010**, *132*, 17667−17669.
(10) Hirata, M.; Gotou, T.; Horiuchi, S.; Fujiwara, M.; Ohba, M. *Carbon* **2004**, *42*, 2929.
(11) Brodie, B. C. *Philos. Trans. R. Soc. London* **1859**, *149*, 249−259.
(12) Dreyer, D. R.; Park, S.; Bielawski, C. W.; Ruoff, R. S. *Chem. Soc. Rev.* **2010**, *39*, 228−240.
(13) Dikin, D. A.; Stankovich, S.; Zimney, E. J.; Piner, R. D.; Dommett, G. H. B.; Evmenenko, G.; Nguyen, S. T.; Ruoff, R. S. *Nature* **2007**, *448*, 457−460.
(14) Rodewald, P. G. U.S. Patent 3,998,270, 1976.
(15) *Standard Handbook of Petroleum & Natural Gas Engineering*; Lyons, W. C., Ed.; Gulf Publishing Co.: Houston, TX, 1996; p 2.
(16) Salas, E.C.; Sun, Z.; Luttge, A.; Tour, J. M. *ACS Nano* **2010**, *4*, 4852−4856.
(17) Segal, M. *Nat. Nanotechnol.* **2009**, *4*, 612−614.
(18) Staudenmaier, L. *Ber. Dtsch. Chem. Ges.* **1898**, *31*, 1481−1487.
(19) Hummers, W. S.; Offeman, R. E. *J. Am. Chem. Soc.* **1958**, *80*, 1339.
(20) Marcano, D. C.; Kosynkin, D. V.; Berlin, J. M.; Sinitskii, A.; Sun, Z.; Slesarev, A.; Alemany, L. B.; Lu, W.; Tour, J. M. *ACS Nano* **2010**, *4*, 4806−4814.
(21) Shen, J.; Hu, Y.; Shi, M.; Lu, X.; Qin, C.; Li, C.; Ye, M. *Chem. Mater.* **2009**, *21*, 3514−3520.
(22) Pham, V. H.; Cuong, V. T.; Hur, S. H.; Oh, E.; Kim, E. J.; Shin, E. W.; Chung, S. K. *J. Mater. Chem.* **2011**, *21*, 3371−3378.
(23) Shen, J.; Shi, M.; Yan, B.; Ma, H.; Li, N.; Hu, Y.; Ye, M. *Colloids Surf., B* **2010**, *81*, 434−438.
(24) Du, D.; Wang, L.; Shao, Y.; Wang, J.; Engelhard, M. H.; Lin, Y. *Anal. Chem.* **2011**, *83*, 746−752.
(25) Pham, T. A.; Kumar, N. A.; Jeong, Y. T. *Synth. Met.* **2010**, *160*, 2028−2036.
(26) Kang, S. M.; Park, S.; Kim, D.; Park, S.Y.; Ruoff, R. S.; Lee, H. *Adv. Funct. Mater.* **2011**, *21*, 108−112.
(27) Rodewald, P. G. U.S. Patent 3,998,270, 1976.
(28) Olley, R. H.; Bassett, D. C. *Polymer* **1982**, *23*, 1707−1710.
(29) American Petroleum Institute, 2003. Recommended Practice for Field Testing of Water-Based Drilling Fluids, 3rd ed.; American Petroleum Institute (01-Nov-2003, 82 pages ANSI/API 13B-1).
(30) Park, S.; Lee, K.; Bozoklu, G.; Cai, W.; Nguyen, S. T.; Ruoff, R. S. *ACS Nano* **2008**, *2*, 572−578.
(31) Bohem, H.P.; Clauss, A.; Fisher, G.; Hofmann, U. *Proceedings of the Fith Conference on Carbon*, 1962.
(32) Schniepp, H. C.; Li, J. L.; McAllister, M. J.; Sai, H.; Herrera-Alonso, M.; Adamson, D. H.; Prud'homme, R. K.; Car, R.; Saville, D. A.; Aksay, I. A. *J. Phys. Chem. B* **2006**, *110*, 8535−8539.
(33) Medhekar, N. V.; Ramasubramaniam, A.; Ruoff, R. S.; Shenoy, V. B. *ACS Nano* **2010**, *4*, 2300−2306.
(34) Gatlin, C. *Petroleum Engineering: Drilling and Well Completions* **1960**, 125.